

# Sigma-1 receptor overexpression promotes proliferation and ameliorates cell apoptosis in $\beta$ -cells

MENGTING KE<sup>1\*</sup>, FENGPING LIN<sup>2\*</sup>, HUAWEI WANG<sup>1</sup>, GUANGZHEN HE<sup>3</sup>,  
JIEYUAN FENG<sup>1</sup>, LINYANG SONG<sup>1</sup>, YANCHENG XU<sup>1</sup> and JIE LIU<sup>1</sup>

<sup>1</sup>Department of Endocrinology, Zhongnan Hospital of Wuhan University, Wuhan, Hubei 430071;

<sup>2</sup>Department of Endocrinology, Xianning Central Hospital, Xianning, Hubei 437100; <sup>3</sup>Department of Pediatrics, Affiliated Taihe Hospital of Hubei University of Medicine, Shiyan, Hubei 442002, P.R. China

Received November 11, 2021; Accepted February 16, 2022

DOI: 10.3892/mmr.2022.12686

**Abstract.** Sigma-1 receptor (Sig-1R) is a class of orphan receptors, the potential role of which in pancreatic islet cells remains poorly understood. The present study aimed to investigate the role of Sig-1R in islet  $\beta$ -cell proliferation and examine the effects of Sig-1R on islet  $\beta$ -cell injury under lipotoxic conditions. Sig-1R-overexpressing MIN6 cells were generated by lentiviral vector transfection. The effect of Sig-1R overexpression on cell proliferation detected by EdU staining, cell cycle progression by propidium iodide (PI), apoptosis by Annexin V-APC/PI, mitochondrial membrane potential by Mitolite Red and cytoplasmic  $\text{Ca}^{2+}$  levels by Fura-2/AM in islet  $\beta$ -cells were measured by flow cytometry. Western blot analysis was used to measure protein expression levels of endoplasmic reticulum (ER) stress markers glucose-regulated protein 78 and C/EBP homologous protein, mitochondrial apoptotic proteins Bcl-2-associated X and Bcl-2 and cytochrome *c*. In addition, ATP levels and insulin secretion were separately measured using ATP Assay and mouse insulin ELISA. Mitochondria-associated ER membrane (MAM) structures in MIN6 cells were then detected using transmission electron microscopy. Protein disulfide isomerase expression and possible colocalization between inositol 1,4,5-trisphosphate receptor and voltage-dependent anion channel 1 were examined using immunofluorescence. Sig-1R overexpression was found to promote  $\beta$ -cell proliferation by accelerating cell cycle progression. Furthermore, Sig-1R overexpression

ameliorated the apoptosis rate whilst impairing insulin secretion induced by palmitic acid by relieving ER stress and mitochondrial dysfunction in MIN6 cells. Sig-1R overexpression also promoted  $\text{Ca}^{2+}$  transport between mitochondria and ER by increasing the quantity of ER adjacent to mitochondria in the 50-nm range. It was concluded that Sig-1R overexpression conferred protective effects on  $\beta$ -cells against lipotoxicity as a result of the promotion of cell proliferation and inhibition of ER stress and oxidative stress, by regulating the structure of MAM.

## Introduction

The global prevalence of diabetes continues to increase every year since 1980 (1). In 2019, ~463 million individuals were diagnosed with diabetes, which accounted for 9.3% of the global adult population (2). Type 2 diabetes mellitus (T2DM) is the most common type of diabetes, where  $\beta$ -cell apoptosis is one of the main causes of T2DM (3). Therefore, further studies on the mechanism underlying  $\beta$ -cell apoptosis are essential for developing treatment strategies for T2DM.

Sigma-1 receptor (Sig-1R) is a class of orphan receptors that has been reported to serve unique physiological functions due to the lack of homology with other mammalian proteins (4,5). Sig-1R agonists has a protective effect on Alzheimer's disease (AD), Parkinson's disease (PD), heart disease, retinal dysfunction, perinatal and traumatic brain injuries, depression and psychostimulant addiction (6). Sig-1R agonists are effective neuroprotective agents (7) and have been applied for treating various neurodegenerative diseases, such as AD, PD and amyotrophic lateral sclerosis (8). In human lens cells, Sig-1R antagonists can inhibit cell proliferation (9), suggesting that Sig-1R can exert regulatory effects on cell proliferation. In addition, Sig-1R receptor agonists have been found to increase the viability of human retinal pigment epithelial cells following oxidative damage (10). Treatment of mice with Sig-1R agonists following transient middle cerebral artery occlusion was reported to improve the extent of cerebral ischemic injury by relieving endoplasmic reticulum (ER) stress (11). Sig-1R receptor agonists can also reduce C/EBP homologous protein (CHOP) expression in HEK cells to attenuate the ER stress-mediated apoptotic pathway (12). Finding from these

---

**Correspondence to:** Dr Yancheng Xu or Dr Jie Liu, Department of Endocrinology, Zhongnan Hospital of Wuhan University, 169 Donghu Road, Wuhan, Hubei 430071, P.R. China  
E-mail: xjl100901@whu.edu.cn  
E-mail: 1070202743@qq.com

\*Contributed equally

**Key words:** apoptosis,  $\beta$ -cell, endoplasmic reticulum stress, mitochondria-associated endoplasmic reticulum membrane, oxidative stress, proliferation, Sigma-1 receptor

previous studies implicated regulatory effects of Sig-1R on ER stress. Since ER stress has been demonstrated to be an important mechanism of islet cell apoptosis in patients with T1DM and T2DM (13,14), it is speculated that Sig-1R activation can also mediate protective effects on islet cells. However, the role of Sig-1R in pancreatic islet cells remains poorly understood. Therefore, the present study investigated the potential link between Sig-1R and islet cell function, by investigating the effects of Sig-1R overexpression on  $\beta$ -cell physiology.

## Materials and methods

**Cell culture.** Pancreatic MIN6 beta-cells were cultured in modified RPMI-1640 (HyClone; Cytiva) containing 11.1 mM glucose and 10% (v/v) FBS (Gibco; Thermo Fisher Scientific, Inc.), 2 mM L-glutamine and 1% penicillin/streptomycin in a humidified atmosphere under 5% CO<sub>2</sub> and 95% air at 37°C.

**Sig-1R overexpression in MIN6 cell lines.** Lentiviral vectors harboring the cloned Sig-1R gene (accession no. NM\_011014) or scrambled sequences were designed and synthesized by Shanghai GeneChem Co., Ltd. The plasmid backbone used was Ubi-MCS-3FLAG-CBh-gcGFP-IRES-puromycin (Shanghai GeneChem Co., Ltd.). Lentivirus packaging was cotransfected with 293T cells of three vectors. A total of 1 ml DNA mixture (target gene GV vector 20  $\mu$ g, Phelper 1.0 vector 15  $\mu$ g, Phelper 2.0 vector 10  $\mu$ g) was prepared and added to 293T cells. The cells were cultured at 37°C for 6 h, then the medium was changed and cultured at 37°C for another 48 h. The supernatant of 293T cells was collected and centrifuged at 4,000 x g at 4°C for 10 min. The supernatant was filtered by 0.45  $\mu$ m filter and centrifuged at 54,000 x g at 4°C for 2 h. After discarding supernatant and resuspending in PBS, centrifugation was continued at 8,600 x g at 4°C for 5 min to obtain supernatant containing lentiviral particles. Suspensions of MIN6 cells during the growth phase were made and counted using a cell counting plate. In total, 2x10<sup>5</sup> cells were inoculated in each well of six-well plates. On day 2, the cells attached the six-well plates before they were transfected with the corresponding lentiviral vectors at a multiplicity of infection of 10. The six-well plates were then gently shaken after adding the virus solution and Hitrans A infection booster solution (Shanghai GeneChem Co., Ltd.) for adequate mixing. The cells were incubated for 8 h at 37°C before the medium was replaced and the cells were incubated for an additional 48 h at 37°C. Subsequently, the cells were cultured at 37°C in a medium containing 10  $\mu$ g/ml puromycin (Biofroxx) to obtain stably transfected cell lines, which were named as Lv-Sig-1R cells and Lv-Ctrl cells. The mRNA and protein expression levels of Sig-1R were measured using reverse transcription-quantitative PCR (RT-qPCR) and western blotting, respectively.

**RT-qPCR.** A EASY spin Cell RNA Rapid Extraction Kit (RN0702, Aidlab) was used to extract the total RNA. The reverse transcription kit ReverTra Ace<sup>TM</sup> qPCR RT Kit (Toyobo Life Science) was used to synthesize double-stranded DNA. The reaction was 65°C for 5 min, then 37°C for 15 min and finally 98°C for 5 min. qPCR was performed using the Magic SYBR Mixture (CoWin Biosciences) in the CFX96 RT-qPCR Detection System (Bio-Rad Laboratories, Inc.). RT-PCR was

programmed as follows: at 95°C for 30 sec, 40 cycles at 95°C for 5 sec, 60°C for 30 sec, and 72°C for 30 sec, and a 5 sec incubation at 65°C. Quantification was controlled by normalization of  $\beta$ -actin. Relative abundance of mRNA expression was calculated by the 2<sup>- $\Delta\Delta$ C<sub>q</sub></sup> method (15). The sequences of primers for PCR were as follows:  $\beta$ -actin forward, 5'-CTGAGAGGGAAATCG TCGT-3' and reverse, 5'-CCACAGGATTCCATACCCAAG A-3' and Sig-1R forward, 5'-TGAGCTTACCACCTACCTCTT TG-3' and reverse, 5'-GGTATACGCTGCTGTCTGAATATG-3'.

**Western blot analysis.** RIPA buffer (Beyotime Institute of Biotechnology) was added to the treated cells to obtain the total protein samples. Protein concentration was then determined by BCA kit (Beyotime Institute of Biotechnology). Then, 10% SDS-PAGE was prepared, subjected to electrophoresis and transferred to PVDF membranes. Blots were blocked with 5% skim milk for 1 h at room temperature, followed by incubation with antibodies separately. The membranes were incubated in the primary antibody overnight at 4°C, washed by TBST containing 0.1% Tween-20 and soaked in the secondary antibody for 1 h at room temperature. The primary antibodies used were as follows: anti- $\beta$ -actin (1:10,000; Abcam; cat. no. ab179467), anti-Sig-1R (1:500; ProteinTech Group, Inc. 15168-1-AP), anti-CHOP (1:1,000; Affinity Biosciences, DF6025), anti-glucose-regulated protein 78 (GRP78) (1:1,000; Affinity Biosciences, AF5366), anti-Bax (1:1,000; Affinity Biosciences, AF0120), anti-Bcl-2 (1:1,000; BIOSS, bs-4563R) and anti-cytochrome *c* (1:5,000; Abcam, ab133504). The secondary antibody used was the goat anti-rabbit conjugated with HRP (1:10,000; Abcam, ab6721). The immunoreactive bands were visualized with an automatic chemiluminescence image analysis system (Tanon 5200, China) The Bandscan 4.3 software (Glyko) was used to analyze the gray value of the protein.

**5-ethynyl-2'-deoxyuridine (EdU) incorporation assay.** A BeyoClick EdU-555 kit (Beyotime Institute of Biotechnology; cat. no. C0075S) was used to measure the proliferation rate of cells. Firstly, 2x10<sup>5</sup> cells were inoculated into a 6-well plate and cultured in a cell incubator overnight at 37°C. EdU was added to the medium so that the final concentration of EdU was 20  $\mu$ M and cells were incubated for another 3 h at 37°C. Subsequently, 4% paraformaldehyde was used to fix the cells for 15 min at indoor temperature and 0.3% Triton X-100 was used for permeabilization. The cells were washed using PBS with 3% BSA (Biofroxx, Germany) twice. The Click Additive solution was then prepared to incubate the cells for 30 min at indoor temperature. The cells were washed again and resuspended in PBS. The fluorescence intensity of 10,000 cells was recorded using a CytoFLEX S flow cytometer (Beckman Coulter, Inc.), before the percentage of EdU-positive cells in each sample was calculated by CytExpert2.3 (Beckman Coulter, Inc.) as follows: FITC positive represents the cells successfully transferred into lentivirus (GFP was detected by FITC). PE-positive represents the EdU-positive cells and PE-negative represents the EdU-negative cells (EdU was detected by PE).

**Cell cycle analysis.** The cells were digested with trypsin before the cell suspension was washed with PBS. Ice-cold 70% ethanol was used to fix the cells overnight. The next

day, the cells were washed twice with PBS. Propidium Iodide (PI)/RNase A (9/1, v/v) (Nanjing KeyGen Biotech Co., Ltd., cat. no. KGA512) staining solution was prepared and added to incubate the cells for 30 min at room temperature. Red fluorescence was then recorded for 10,000 cells at 488 nm using the CytoFLEX S flow cytometer (Beckman Coulter, Inc.). Since the DNA content is different during different phases of the cell cycle, the fluorescence intensity detected by the flow cytometer would also be expected to be different by CytExpert 2.3 (Beckman Coulter, Inc.). Therefore, the number of cells in the three different phases (G<sub>1</sub>, S and G<sub>2</sub> phases) of the cell cycle was obtained.

**Determination of cell apoptosis.** An Annexin V-APC/PI apoptosis detection kit (Nanjing KeyGen Biotech Co., Ltd. KGA1030) was used to detect the cell apoptosis rate. After the cells were digested with trypsin, 5  $\mu$ l Annexin V-APC and 5  $\mu$ l PI dyes were added to cell suspension. The cell apoptosis rate was detected using the CytoFLEX S flow cytometer (Beckman Coulter, Inc.) after 1 h incubation at indoor temperature. A total of 10,000 cells were recorded and the results were analyzed by CytExpert 2.3 (Beckman Coulter, Inc.) as follows: Annexin V-APC-positive and PI-negative, early apoptotic cells; Annexin V-APC-positive and PI-positive, late apoptotic cells. Cell apoptosis rate=(early apoptosis + late apoptosis)/total number of cells per well.

**Insulin secretion assay.** A total of  $2 \times 10^5$  cells was seeded into 6-well plates. The next day, palmitic acid (PA; Sigma-Aldrich; Merck KGaA) was added to incubated for 24 h at 37°C after the cells adhered to the wall. And then, the cells were rinsed with PBS once and RPMI-1640 (HyClone; Cytiva) without glucose was added and incubated for 30 min at 37°C. HEPES-buffered Krebs-Ringer bicarbonate buffer (KRBB) (16) containing 0.1% BSA and 2.5 mmol/l glucose was then added for incubation for 1 h at 37°C. The supernatant was collected for the detection of basal insulin secretion. Subsequently, KRBB solution containing 0.1% BSA and 20 mmol/l glucose was added and incubated for 1 h at 37°C. The supernatant was then collected to detect insulin secretion after glucose stimulation. The insulin concentration was measured using a mouse insulin ELISA kit (Elabscience Biotechnology Inc. PI602).

**Measurement of adenosine triphosphate (ATP) production.**  $2 \times 10^5$  cells were seeded into 6-well plates. The next day, PA was added to incubated for 24 h at 37°C after the cells adhered to the wall. Afterwards, ATP generation was measured using an ATP Assay Kit (Beyotime Institute of Biotechnology, cat. no. S0026). The cells were lysed, and the supernatant was obtained after centrifugation at 12,000 x g at 4°C for 5 min. The standard curve was established using ATP standard solution. The working fluid was configured and finally the ATP concentration was measured in a multi-purpose microplate reader (Enspire; PerkinElmer, Inc.).

**Measurement of mitochondrial membrane potential (MMP).** Cell Meter™ Kit (ATT Bioquest, Inc., 22806) was used to detect the MMP. The cell suspension was prepared and 1  $\mu$ l 500X MitoTell Red was added to the 0.5 ml cell solution. The cells were then incubated at 37°C under 5% CO<sub>2</sub> for 30 min,

before they were precipitated at 200 x g at 4°C for 5 min and resuspended in 0.5 ml detection buffer. The cells were finally analyzed using the cytoFLEX S flow cytometer (Beckman Coulter, Inc.). A total of 10,000 cells were recorded, and the average fluorescence intensity value of each sample was calculated by CytExpert 2.3 (Beckman Coulter, Inc.).

**Transmission electronic microscopy (TEM).** Lv-Sig-1R cells and Lv-Ctrl cells were fixed with an electron microscope stationary liquid (2.5% Glutaraldehyde (Solarbio, China, P1126) for 1 h at 4°C, before an ascending ethyl alcohol gradient was used for dehydration. The cells were permeated overnight at 37°C using SPI-Pon 812 (SPI, America, 90529-77-4) and polymerized in oven at 60°C for 48 h. After cutting into slices of 60-80 nm, the cells were stained using uranium-lead double staining (2% uranium acetate and 2.6% lead citrate) for 15 min at room temperature. The images were analyzed using a transmission electron microscope. Mitochondria and ER were delimited using Image-pro plus 6.0 (National Institutes of Health) before the fraction of the mitochondrial membrane in contact with ER within a 50-nm range was marked (17).

**Immunofluorescence.**  $2 \times 10^5$  cells was first seeded onto the coverslip in 6-well plates. The next day, 0.5 mM PA was added to incubated for 24 h at 37°C after the cells adhered to the coverslip before 4% paraformaldehyde was used to fix the cells for 30 min at indoor temperature and PBS was used to wash them. The membrane breaking solution (1% Triton X-100) and 3% hydrogen peroxide solution were added to incubate the cells for 30 min at room temperature, before PBS was used to wash the cells again. Then they were blocked with 5% BSA (Biofroxx, Germany) for 10 min at room temperature. Next, the cells were incubated in the primary antibody overnight and washed and soaked in the secondary antibody for 50 min at indoor temperature. The primary antibodies used were as follows: Anti-protein disulfide isomerase (PDI; 1:200; Proteintech Group, Inc. 66422-1-1 g), anti-inositol 1,4,5-trisphosphate receptor (IP3R; 1:100; ABclonal Biotech Co., Ltd. A4436), and anti-voltage-dependent anion channel 1 (VDAC1; 1:100; ABclonal Biotech Co., Ltd., A19707). The secondary antibody used was the goat anti-mouse conjugated with Cy3 (1:50; cat. no. AS-1111; Wuhan Aspen Biotechnology Co., Ltd.) and Cy5 (1:200; Wuhan Bioqiandu Technology Co., Ltd.; cat. no. B100810). Finally, 100  $\mu$ l 10  $\mu$ g/ml DAPI per well was added to incubate cells for 5 min at room temperature. After washing the cells with PBS, the coverslips were sealed by anti-fade mounting medium (Biosharp; cat. no. BL701A) and the cells were observed under a fluorescence at 400 magnification or confocal microscope at 630 magnification.

**Cell calcium detection.** Fura-2/AM (ATT Bioquest, Inc.) was used to detect the intracellular cell calcium levels. A 4 mM stock solution was prepared by dissolving Fura-2/AM in DMSO. This Fura-2/AM dye was then diluted to a 4  $\mu$ M working solution using D-Hank's buffer (Biosharp, BL559A). A total of  $2 \times 10^5$  cells were seeded into 6-well plates. The next day, 0.5 mM PA was added to incubated for 24 h at 37°C after the cells adhered to the wall. The medium in pre-cultured cells was first removed and the cells were washed three times with Hank's buffer. The Fura-2/AM dye was then added to the cells for 60 min at 37°C

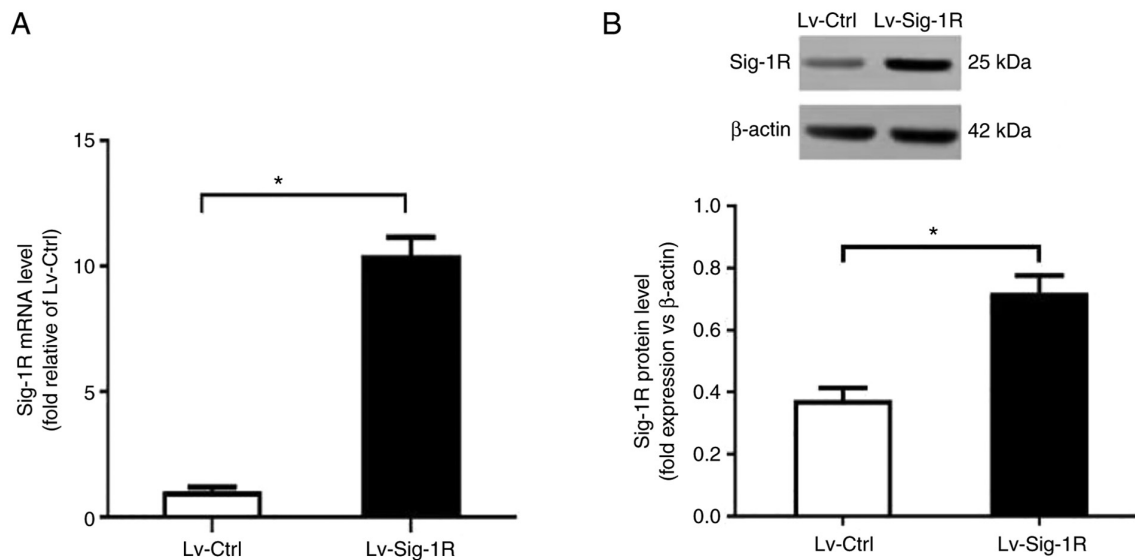


Figure 1. Establishment of Sig-1R-overexpressing MIN6 cells. (A) Sig-1R mRNA and (B) protein expression in Lv-Sig-1R and Lv-Ctrl cells were measured. The results are means  $\pm$  SD from three experiments. \* $P < 0.05$ . Sig-1R, Sigma-1 receptor; Lv, lentiviral; Ctrl, control.

before the dye was removed. The cells were then washed three times with Hank's buffer. Finally, the cells were processed using a cytoFLEX S flow cytometer (Beckman Coulter, Inc.) in UV excitation (405/10) (channel 505-545 nm, dye KO525). A total of 10,000 cells were recorded and the average fluorescence intensity value of each sample was calculated by CytExpert 2.3 (Beckman Coulter, Inc.). Fura-2/AM is a calcium fluorescence probe, which can specifically bind cytoplasmic  $\text{Ca}^{2+}$  (binding ratio is 1:1). The increase or decrease of fluorescence signal can indicate that the treatment causes the increase or decrease of intracellular calcium. The average fluorescence intensity can reflect the changes of the overall calcium level of cells.

**Statistical analysis.** The results were expressed as the mean  $\pm$  standard deviation of three experimental repeats. All data were analyzed using the SPSS20.0 software (IBM Corp). Graphs were drawn using GraphPad Prism 8 software (Graphpad Software, Inc.). Statistical significance between two experimental conditions was analyzed using the Student's *t* test whereas two-way ANOVA followed by Sidak's post hoc test was used for comparisons among >two groups.  $P < 0.05$  was considered to indicate a statistically significant difference.

## Results

**Generation of Sig-1R-overexpressing cells.** Lentiviral vectors were used to transfect MIN6 cells to create the Sig-1R-overexpressing Lv-Sig-1R cells. RT-qPCR revealed a significant increase in Sig-1R mRNA expression in Lv-Sig-1R cells compared with that in the Lv-control cells ( $P < 0.05$ ; Fig. 1A). Subsequent western blot analysis also showed a significant increase in Sig-1R protein expression in Lv-Sig-1R cells compared with that in Lv-control cells ( $P < 0.05$ ; Fig. 1B).

**Sig-1R overexpression promotes proliferation and cell cycle progression.** EdU incorporation assay showed that Lv-Sig-1R cells had a significantly increased percentage of EdU-positive cells compared with that in the Lv-Ctrl cells

( $P < 0.05$ ; Fig. 2A and B), suggesting that Sig-1R overexpression promoted MIN6 cell proliferation. Cell cycle analysis demonstrated that the percentage of cells in  $G_1$  phase was significantly decreased whereas that in S phase was significantly increased, in Lv-Sig-1R cells compared with that in Lv-Ctrl cells ( $P < 0.05$ ; Fig. 2C and D). These results suggest that Sig-1R overexpression promoted  $\beta$ -cell proliferation resulting from the potentiation of cell cycle progression.

**Sig-1R overexpression prevents apoptosis and impairs PA-induced insulin secretion in MIN6 cells.** Cell apoptosis assay revealed similar cell apoptosis rates under basal conditions in both Lv-Ctrl and Lv-Sig-1R cells. However, the apoptosis rate significantly increased after PA was added in both groups of these cells ( $P < 0.05$ ; Fig. 3). In particular, the cell apoptosis rate increased by a larger extent in Lv-Ctrl cells compared with that in Lv-Sig-1R cells after exposure to PA ( $P < 0.05$ ; Fig. 3).

Glucose-stimulated insulin secretion assay showed that insulin secretion was significantly decreased in Lv-Ctrl and Lv-Sig-1R cells after exposure to PA compared with that in their corresponding control that were not treated with PA ( $P < 0.05$ ; Fig. 4A). However, significantly increased insulin secretion was observed in Sig-1R-overexpressing MIN6 cells compared with that in Lv-Ctrl cells regardless of whether they were exposed to palmitate ( $P < 0.05$ ; Fig. 4A). Therefore, it was concluded that Sig-1R overexpression ameliorated PA-induced impaired insulin secretion and cell apoptosis.

**Sig-1R overexpression relieves ER stress and mitochondrial dysfunction induced by PA in MIN6 cells.** GRP78 and CHOP are typical markers of ER stress (18). The results in the present study showed that the protein expression of GRP78 and CHOP in Lv-Ctrl and Lv-Sig-1R cells was both significantly increased on exposure to PA compared with that in their corresponding cells not treated with PA ( $P < 0.05$ ; Fig. 4C). Similar to the insulin secretion data, after treatment with cells with treated with PA, protein expression of GRP78 and

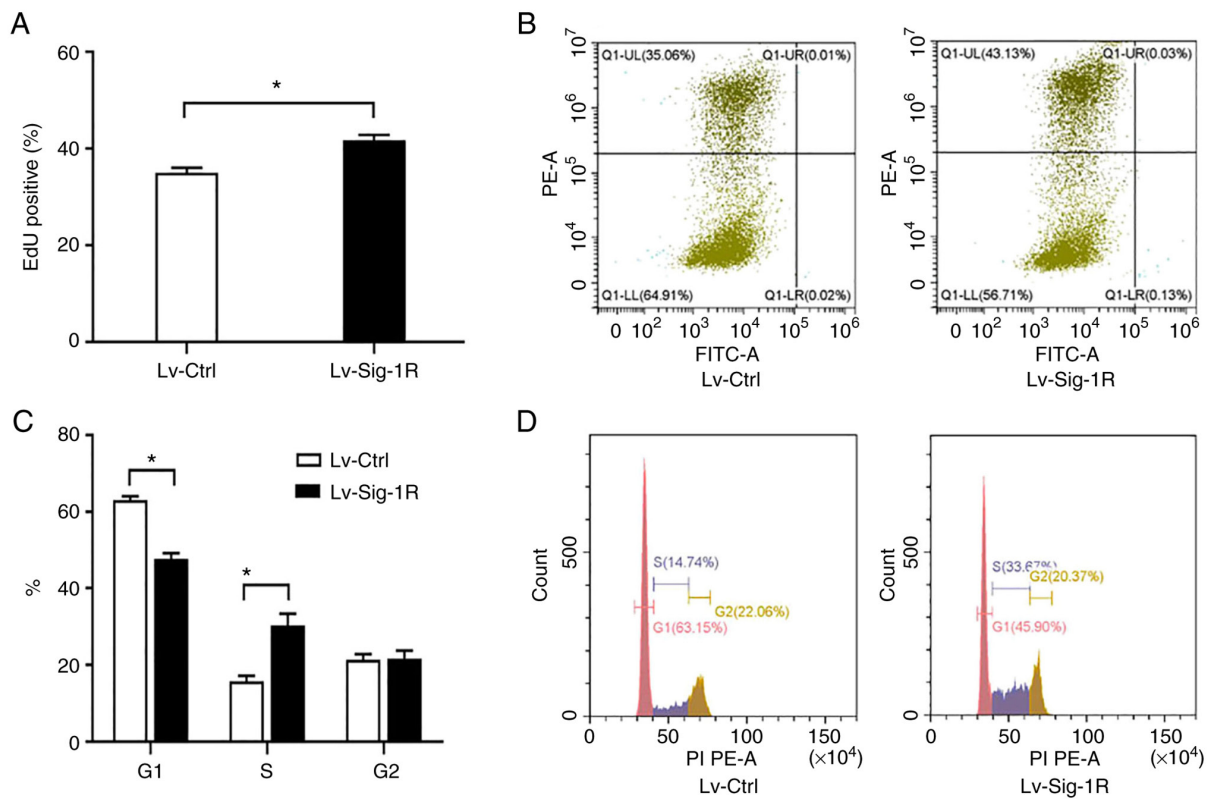


Figure 2. Effect of Sig-1R overexpression on MIN6 cell proliferation and cell cycle progression. (A) Quantification of the percentage of EdU-positive cells in Lv-Sig-1R cells and Lv-Ctrl cells. (B) Representative flow cytometry diagrams showing the percentage of EdU-positive cells (Q1-UL represents the EdU-positive cells and Q1-LL represents the EdU-negative cells. GFP was detected by FITC and EdU was detected by PE). (C) Quantification of the percentage of cells in the three different phases of cell cycle in Lv-Sig-1R cells and Lv-Ctrl cells. (D) Representative flow cytometry histograms showing the percentage of cells in the different cell cycle phases. The results represent the means  $\pm$  SD from three experiments. \* $P < 0.05$ . Sig-1R, Sigma-1 receptor; Lv, lentiviral; Ctrl, control.

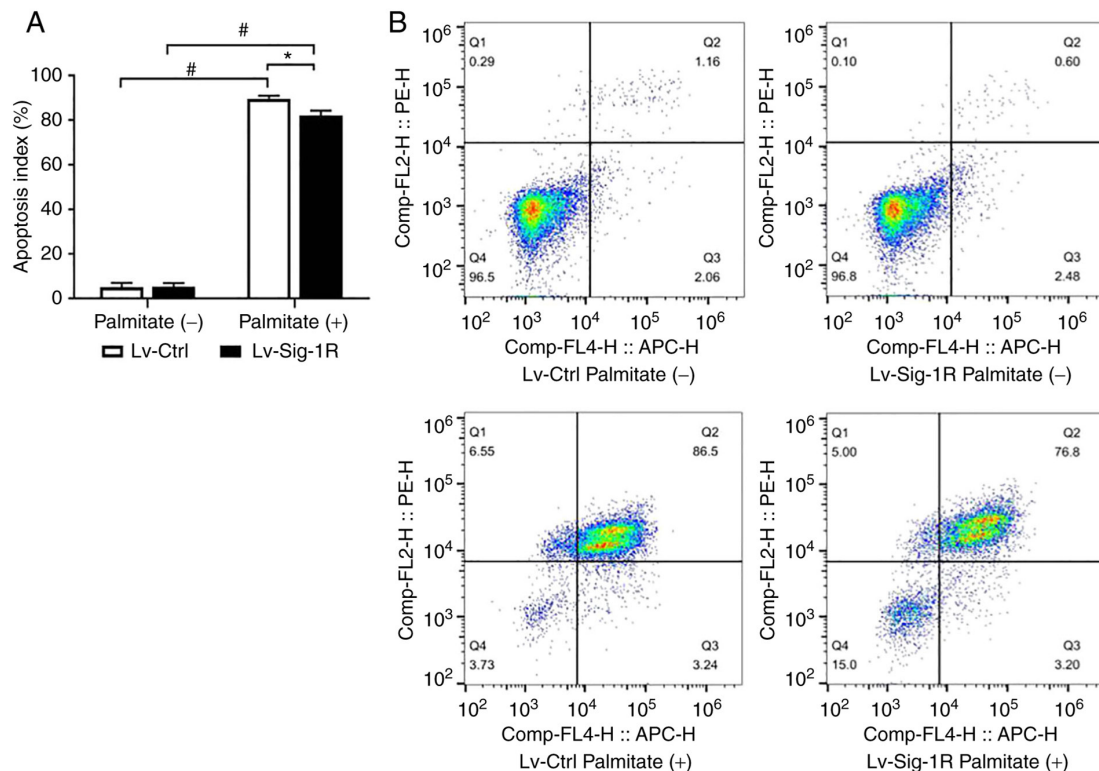


Figure 3. Effect of Sig-1R overexpression on palmitate-induced MIN6 cell apoptosis. (A) Quantification of the cell apoptosis rate in Lv-Sig-1R cells and Lv-Ctrl cells. (B) Representative flow cytometry diagrams showing the cell apoptosis rate. Q2 represents late apoptotic cells and Q3 represents early apoptotic cells. The results represent the means  $\pm$  SD from three experiments. \* $P < 0.05$  and # $P < 0.05$ . Sig-1R, Sigma-1 receptor; Lv, lentiviral; Ctrl, control.



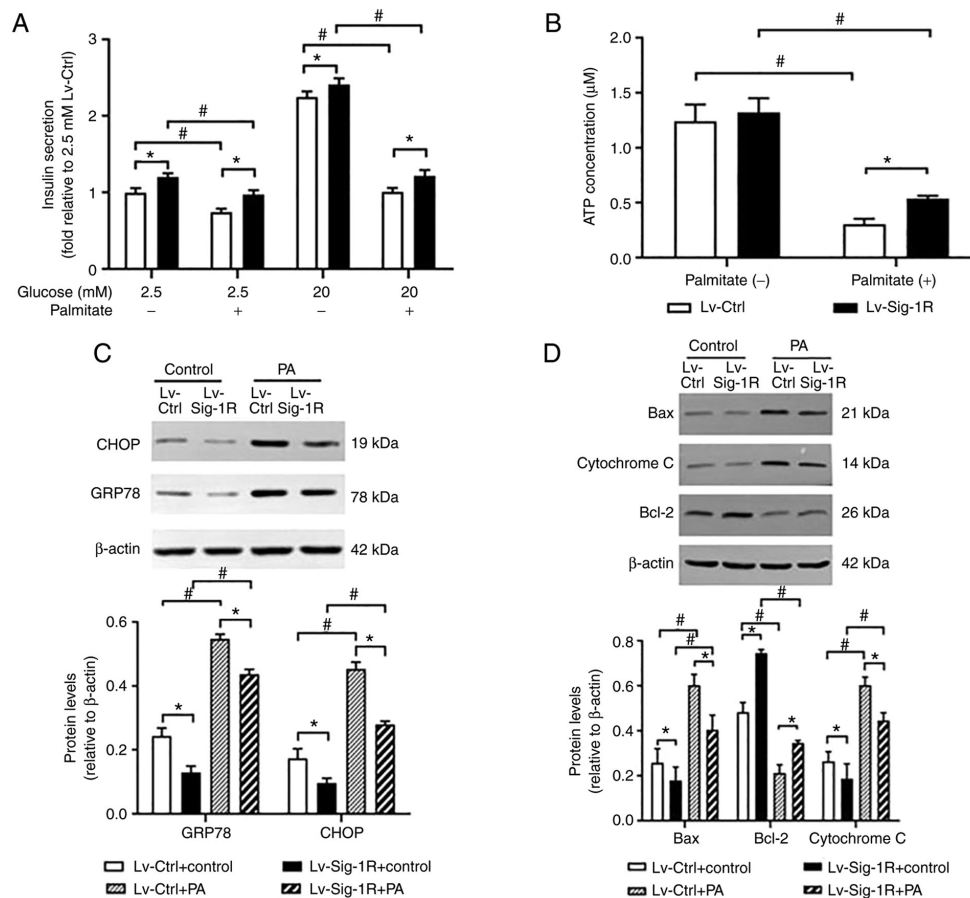


Figure 4. Effect of Sig-1R overexpression on PA- and glucose-induced insulin secretion, ATP production and ER stress in MIN6 cells. (A) Levels of insulin secretion by Lv-Sig-1R cells and Lv-Ctrl cells. (B) Levels of ATP production by Lv-Sig-1R cells and Lv-Ctrl cells. (C) Levels of GRP78 and CHOP protein expression in Lv-Sig-1R cells and Lv-Ctrl cells. (D) Expression of mitochondria-associated apoptotic proteins Bax, Bcl-2 and Cytochrome *c* in Lv-Sig-1R cells and Lv-Ctrl cells. The results are means  $\pm$  SD for three observations; \* $P$ <0.05 and # $P$ <0.05. ER, endoplasmic reticulum; GRP78, glucose-regulated protein 78; CHOP, C/EBP homologous protein; Sig-1R, Sigma-1 receptor; Lv, lentiviral; Ctrl, control; PA, palmitic acid.

CHOP was significantly decreased in Sig-1R-overexpressing MIN6 cells compared with that in Lv-Ctrl cells ( $P$ <0.05; Fig. 4C). PDI promotes the correction of disulfide bonds between proteins. During the early stages of ER stress, PDI is typically activated to maintain ER stability by reducing the aggregation of misfolded and unfolded proteins within ER (19). Immunofluorescence results showed that PDI expression was markedly decreased in Sig-1R-overexpressing MIN6 cells compared with that in Lv-Ctrl cells following the exposure of both cells to PA (Fig. 5). These results suggest that Sig-1R overexpression can relieve ER stress induced by PA in MIN6 cells.

During oxidative stress, Bax and cytochrome *c* are released from mitochondria into cytoplasm and activate caspase 9 to induce apoptosis, suggesting that Bax and cytochrome *c* are mitochondria-associated apoptosis proteins (20). Downstream, ATP and MMP can be used to reflect mitochondrial function. After PA intervention, Bax and cytochrome *c* protein levels were significantly increased, whilst ATP, MMP and Bcl-2 expression were significantly decreased. Bax and cytochrome *c* expression were significantly increased in the Sig-1R overexpression group (Fig. 4D), whereas ATP (Fig. 4B), MMP (Fig. 6) and Bcl-2 expression levels (Fig. 4D) were significantly decreased ( $P$ <0.05) compared with that in Lv-Ctrl cells following the exposure of both cells to PA. Therefore,

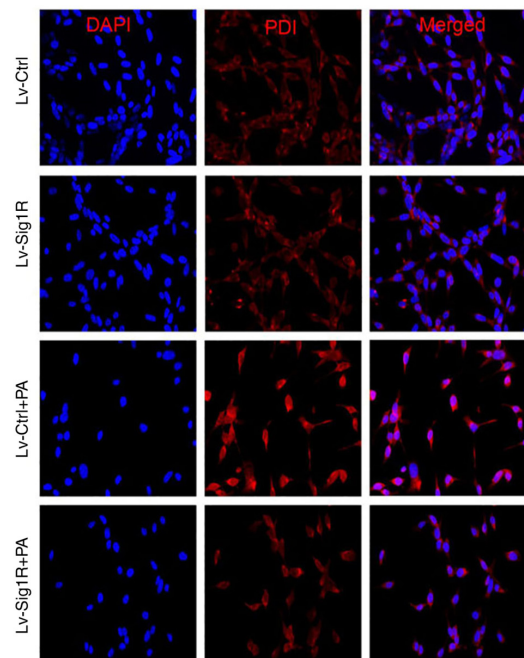


Figure 5. Effect of Sig-1R overexpression on PDI expression in MIN6 cells. Representative images of PDI expression by immunofluorescence in Lv-Sig-1R and Lv-Ctrl cells. Magnification,  $\times 400$ . Sig-1R, Sigma-1 receptor; Lv, lentiviral; Ctrl, control; PA, palmitic acid; PDI, protein disulfide isomerase.

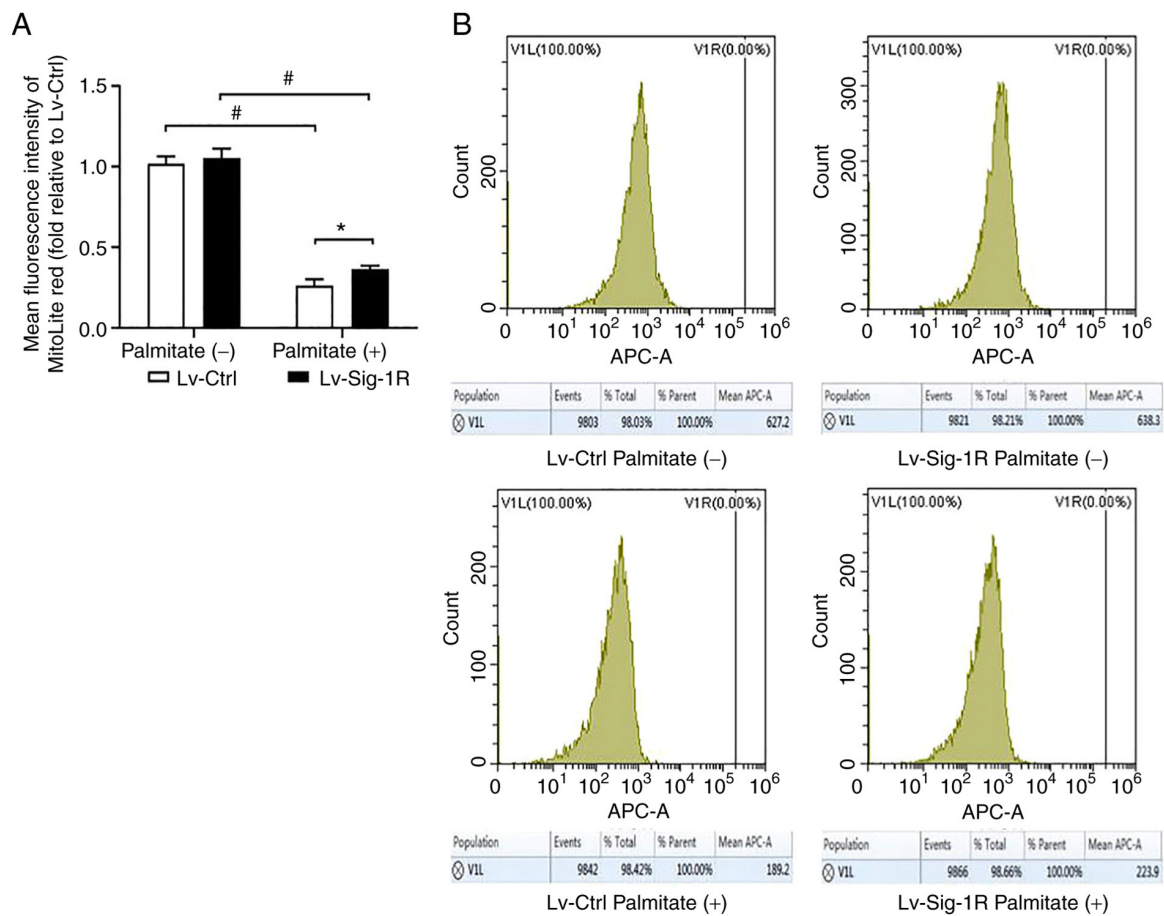


Figure 6. Effect of Sig-1R overexpression on the mitochondrial membrane potential in MIN6 cells. (A) Quantification of mitochondrial membrane potential levels in Lv-Sig-1R cells and Lv-Ctrl cells. (B) Representative flow cytometry histogram showing the average fluorescence intensity of Mitolite Red, which is the fluorescent probe used to detect the mitochondrial membrane potential level. The results are shown as the means  $\pm$  SD from three experiments. \* $P < 0.05$  and # $P < 0.05$ . Sig-1R, Sigma-1 receptor; Lv, lentiviral; Ctrl, control.

these results suggest that Sig-1R overexpression alleviated PA-induced mitochondrial dysfunction.

*Sig-1R overexpression alters the structure of mitochondria-associated membranes (MAM).* Mitochondrial and ER are important organelles within nucleated eukaryotic cells that are key to intracellular cell physiology. They are arranged in parallel, where various points of physical coupling exists between the outer mitochondrial membrane and the ER, which are called the MAM (21). The MAM contains a plethora of functional proteins that regulate the transport of metabolites and signaling molecules, such as Sig-1R (22). Therefore, it was hypothesized that Sig-1R overexpression may alter the structure of MAM. The present study next examined the structure of MAM using TEM. An increase in the quantity of ER adjacent to mitochondria was observed in the 50-nm range according to TEM analysis in Lv-Sig-1R cells compared with that in Lv-control cells (Fig. 7). Subsequently, immunofluorescence was used to detect the effect of Sig-1R overexpression on the expression and localization of key MAM proteins IP3R and VDAC1. The expression level of VDAC1 was markedly increased in Sig-1R-overexpressing MIN6 cells compared with that in Lv-control cells without PA. Although the expression level of the two proteins decreased in the PA group, VDAC1 expression remained to be higher in Sig-1R-overexpressing

MIN6 cells. On the other hand, Sig-1R overexpression had no significant effect on IP3R protein expression with or without PA compared with that in Lv-control cells (Fig. 8). These results suggested that Sig-1R overexpression had an effect on the structure of MAM by increasing the expression of VDAC1.

*Sig-1R overexpression increases cytoplasmic calcium level.* Fura 2/AM is a class of cytoplasmic calcium probe that can be used to reflect cytoplasmic calcium levels. The present study revealed that the cytoplasmic calcium level was significantly increased in the PA group compared with that in the group not treated with PA in both Lv-control and Lv-Sig-1R cells (Fig. 9). In addition, the cytoplasmic calcium level was found to be significantly lower in Sig-1R-overexpressing cells compared with that in control cells in the absence of PA (Fig. 9).

## Discussion

Sig-1R is a class of receptors that have unique pharmacological effects and chaperone activity (23). In human lens cells, Sig-1R receptor antagonists have been shown to inhibit cell proliferation (9). In the present study, Sig-1R overexpression was found to increase the proliferation rate of MIN6 cells. Cell cycle progression serves a key role in regulating cell proliferation, where the transition from  $G_0/G_1$  to the S phase is a key step in this

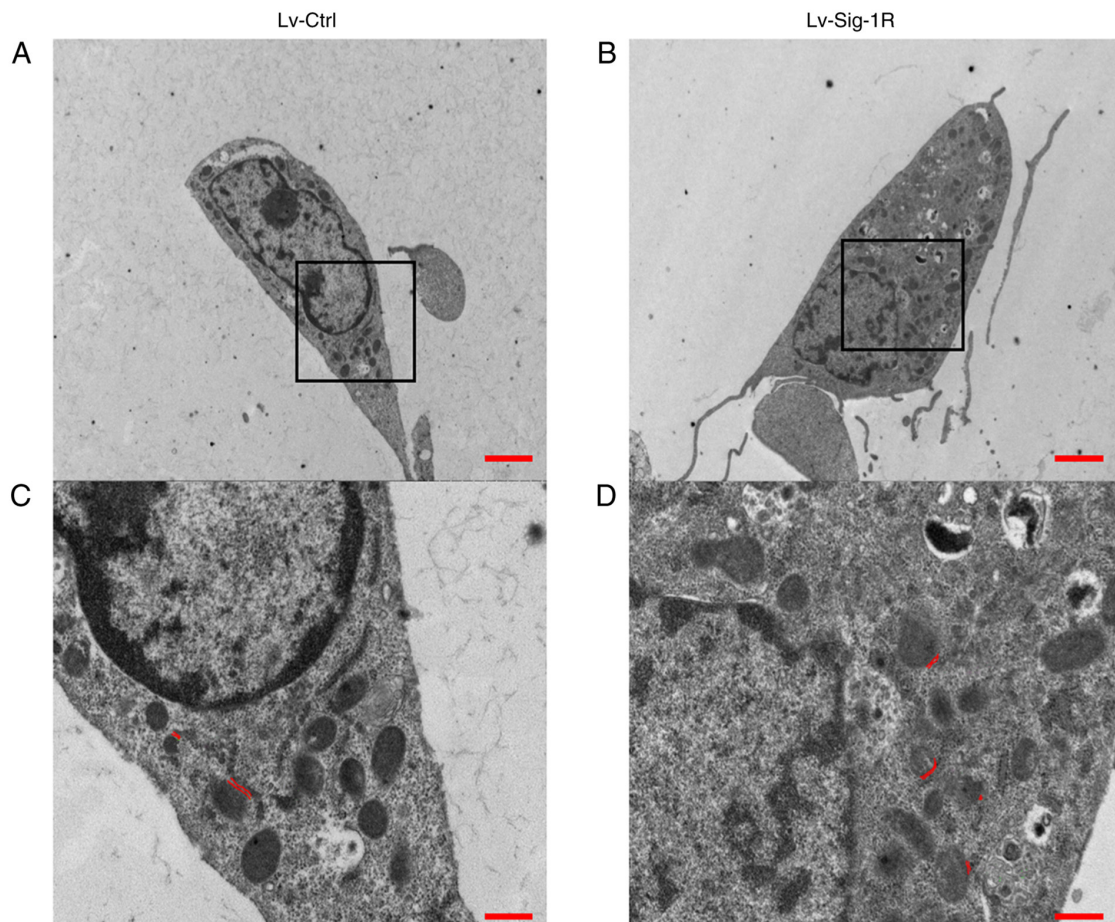


Figure 7. Effect of Sig-1R overexpression on the mitochondria-endoplasmic reticulum junction morphology. Representative transmission electron microscopy images of the whole cell for (A) Lv-Ctrl cells and (B) Lv-Sig-1R cells. Scale bars, 20  $\mu$ m. Representative images of the amplified sections for (C) Lv-Ctrl cells and (D) Lv-Sig-1R cells of the corresponding black box content in (A) and (B), respectively. Scale bars, 5  $\mu$ m. The double red line shows the location of the mitochondria-endoplasmic reticulum coupling structure in the range of 50 nm. Sig-1R, Sigma-1 receptor; Lv, lentiviral; Ctrl, control.

process (24). To explore the mechanism further, the cell cycle progression analysis of MIN6 cells in the present study revealed that Sig-1R overexpression this process, specifically from the G<sub>1</sub> to the S phase. Therefore, it was hypothesized that Sig-1R can promote cell proliferation by positively regulating the cell cycle.

Numerous studies have shown that exposure to PA can decrease insulin secretion and induce apoptosis in  $\beta$ -cells (25,26). Apoptosis and Glucose-stimulated insulin secretion assays in the present study also showed that exposure to PA increased apoptosis whilst decreasing insulin secretion, which was consistent with these previous findings (25,26). In addition, Sig-1R overexpression was found to ameliorate apoptosis and restored the insulin secretion previously impaired by PA in MIN6 cells. Sig-1R agonists have been previously shown to alleviate cerebral ischemia-reperfusion injury by reversing neuronal apoptosis and improving neurological function (27). Amyotrophic lateral sclerosis is a progressive neurological disorder (28). In this disease, brain neuronal apoptosis was found to be inhibited after prolonged treatment with Sig-1R agonists (28). Altogether, these findings suggest that Sig-1R mediates protective effects against cell damage, whereby increasing Sig-1R activity can alleviate cell damage.

Therefore, the underlying mechanism was explored. Oxidative and ER stress are associated with islet  $\beta$ -cell dysfunction and participate in the development of T2DM (29).

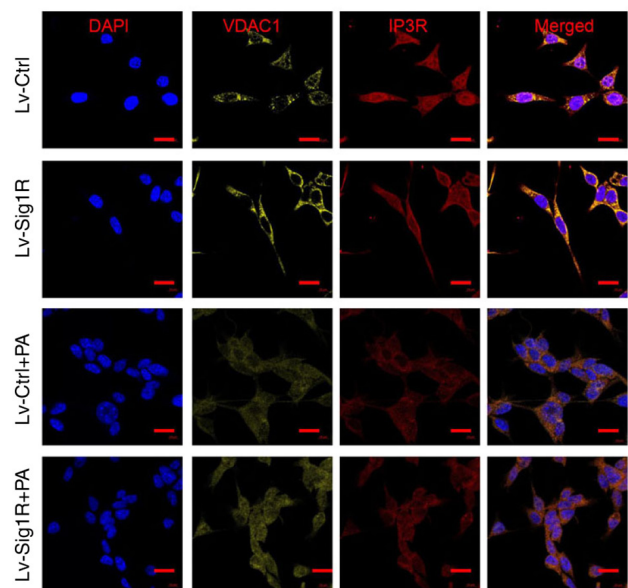


Figure 8. Effect of Sig-1R overexpression on the mitochondria-associated ER membrane junction morphology. Representative immunofluorescence images of IP3R-VDAC1 on the mitochondria-associated ER membrane in Lv-Sig-1R cells with Lv-Ctrl cells, which was imaged using confocal microscopy. Scale bars, 10  $\mu$ m. PA, palmitic acid; IP3R, inositol 1,4,5-triphosphate receptor; VDAC, voltage-dependent anion channel 1; Sig-1R, Sigma-1 receptor; Lv, lentiviral; Ctrl, control.



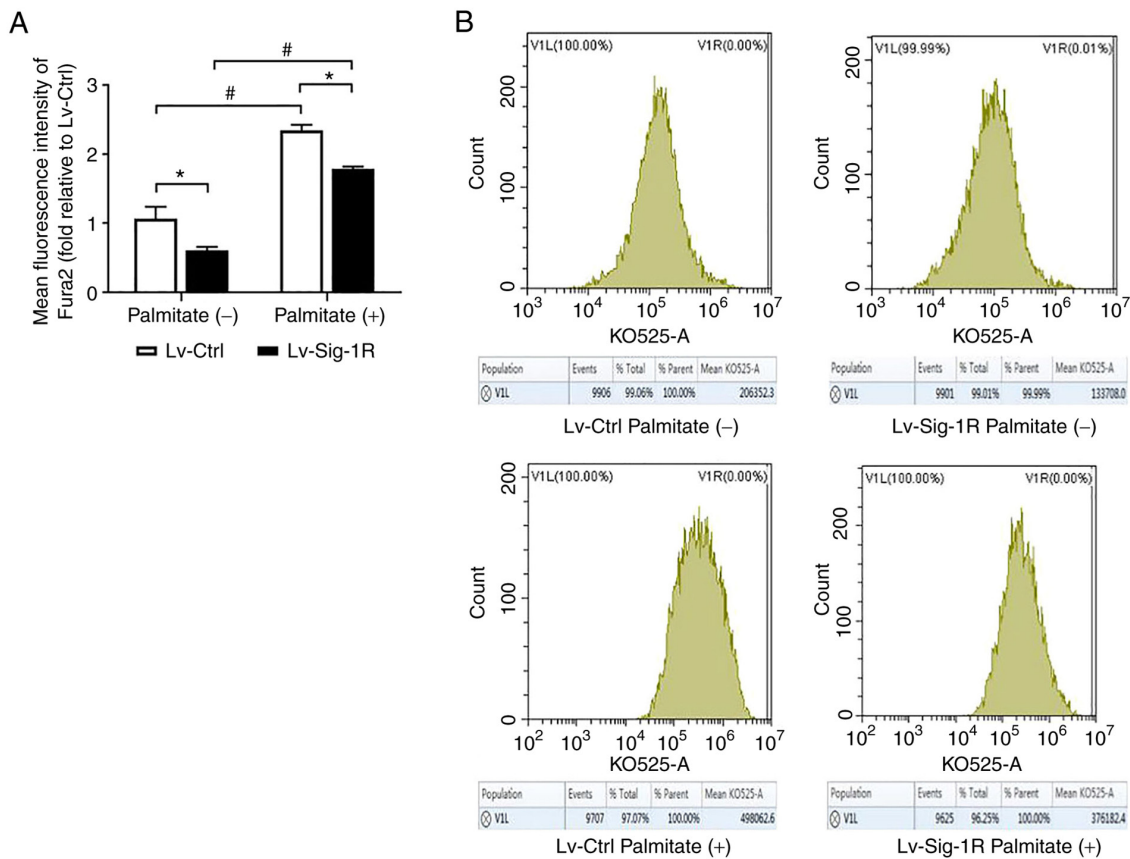


Figure 9. Effect of Sig-1R overexpression on the intracellular calcium levels of MIN6 cells. (A) Quantification of cytoplasmic calcium levels in Lv-Sig-1R cells and Lv-Ctrl cells. (B) Representative flow cytometry histograms showing the average fluorescence intensity of Fura 2, which is a fluorescent probe used to detect cytoplasmic calcium levels. The results are representative of the mean  $\pm$  SD of three experimental repeats. \* $P < 0.05$  and # $P < 0.05$ . Sig-1R, Sigma-1 receptor; Lv, lentiviral; Ctrl, control.

Results in the present study showed that Sig-1R overexpression relieved PA-induced ER stress in MIN6 cells by decreasing the protein expression of the ER chaperone GRP78 and the ER pro-apoptotic molecule CHOP. Previous studies also reported that Sig-1R serves important roles in ER stress (11,30). Sig-1R upregulation was found to alleviate neuronal damage caused by ER stress (11), whereas the activation of Sig1R effectively inhibited the expression of GRP78 and CHOP to alleviate apoptosis in mouse hippocampal cells (30). PDI promotes the formation of correct disulfide bonds between and/or within proteins (31). During the early stages of ER stress, PDI is activated to maintain stability by reducing the aggregation of misfolded and unfolded proteins within ER (19). The present showed that PDI expression was decreased in the Sig-1R-overexpressing MIN6 cells compared with that in Lv-Ctrl cells after exposure to PA. Taken together, these findings suggested that Sig-1R overexpression can relieve MIN6 cell apoptosis under lipotoxic conditions through ameliorating ER stress. Furthermore, the present study also concluded that Sig-1R overexpression can alleviate PA-induced mitochondrial dysfunction in MIN6 cells. Previous studies showed that Sig1R agonists relieve oxidative stress (32) and promote ATP production (33). Tagashira *et al* (34) found that ligands that can activate Sig-1R can protect cardiomyocytes by increasing IP3R-mediated mitochondrial ATP production. Therefore, Sig-1R overexpression was concluded to ameliorate apoptosis and restore insulin secretion under lipotoxic

conditions by relieving ER stress and mitochondrial dysfunction in MIN6 cells.

Mitochondrial and ER are important organelles in eukaryotic cells. Although the two organelles are normally in close proximity to each other, their membranes do not fuse (35). Therefore, both can retain their own unique structure and function (35). MAM is the site of physical coupling between the mitochondrial outer membrane and ER, where Sig-1R has been reported to be a chaperone protein (22). Sig-1R knockdown can lead to AD, the mechanism of which may be associated with the loss of MAM integrity (36). Therefore, it was speculated in the present study that Sig-1R can regulate the MAM structure in islet cells, thereby attenuating islet apoptosis by regulating MAM structure by regulating ER stress and mitochondrial function. An increase in the number of ER and mitochondria contacts was observed in the 50-nm range by TEM analysis in Lv-Sig-1R cells, suggesting that Sig-1R overexpression serves an important role in promoting the formation of MAM.

IP3R is one of the calcium release channels in the ER (37). When IP3R interacts with VDAC1 on the outer mitochondrial membrane using the molecular chaperone glucose regulatory protein 75 (GRP75) bridge, calcium ions are released from the ER directly through IP3R without the combination between IP3 and IP3R (38). The IP3R/GRP75/VDAC1 complex is a multi-protein structure that is associated with the coupling of the mitochondrial cytoplasmic network, where GRP75 knockdown can prevent MAM formation and reduce mitochondrial

calcium uptake (39). Immunofluorescence results from the present study showed that Sig-1R overexpression mainly increased the expression levels of VDAC1. This suggests that Sig-1R mediated a regulatory effect on the structure of MAM by increasing the expression of VDAC1.

MAM enables the direct transport of ER calcium to the mitochondria through the IP3R/GRP75/VDAC1 complexes (40). Sig-1R has been shown to control calcium transport by regulating the formation of these complexes (41). The present study showed that the cytoplasmic calcium levels were decreased in Sig-1R-overexpressing MIN6 cells compared with that in Lv-Ctrl cells. This may have been because Sig-1R overexpression increased direct calcium transport from the ER to the mitochondria by increasing the number of mitochondria-ER coupling sites, which in turn reduced calcium leakage into the cytosol. Therefore, it was also speculated that Sig-1R overexpression ameliorated ER stress and mitochondrial dysfunction in MIN6 cells by preserving calcium transport between the mitochondria and ER.

To conclude, the present study revealed that Sig-1R overexpression may exert protective effects on  $\beta$ -cells under lipotoxic condition. This could be because Sig-1R overexpression not only promoted cell proliferation but also relieved ER stress and mitochondrial dysfunction. However, several limitations remain. Only one cell line was used. It should be verified further in primary  $\beta$ -cells or in  $\beta$ -cells *in vivo*. The specific mechanism of how Sig-1R regulates cell apoptosis require further investigation, such that cleaved caspase 3 expression levels should be tested.

## Acknowledgements

Not applicable.

## Funding

The present study was supported by the National Natural Science Foundation of China (grant no. 81970718).

## Availability of data and materials

The datasets used and/or analyzed during the current study are available from the corresponding author on reasonable request.

## Authors' contributions

MK, YX and JL contributed to conception and design of the study. MK and FL performed the experiments and data collection. HW, GH, JF and LS contributed to analysis and interpretation of data. YX and JL revised the manuscript for important intellectual content. MK and FL confirm the authenticity of all the raw data. All authors have read and approved the final manuscript.

## Ethics approval and consent to participate

Not applicable.

## Patient consent for publication

Not applicable.

## Competing interests

The authors declare that they have no competing interests.

## References

1. Saeedi P, Petersohn I, Salpea P, Malanda B, Karuranga S, Unwin N, Colagiuri S, Guariguata L, Motala AA, Ogurtsova K, *et al*: Global and regional diabetes prevalence estimates for 2019 and projections for 2030 and 2045: Results from the international diabetes federation diabetes Atlas, 9th edition. *Diabetes Res Clin Pract* 157: 107843, 2019.
2. International Diabetes Federation: IDF Diabetes Atlas. 9th edition. 2019.
3. Butler AE, Janson J, Bonner-Weir S, Ritzel R, Rizza RA and Butler PC: Beta-cell deficit and increased beta-cell apoptosis in humans with type 2 diabetes. *Diabetes* 52: 102-110, 2003.
4. Ramachandran S, Lu H, Prabhu U and Ruoho AE: Purification and characterization of the guinea pig sigma-1 receptor functionally expressed in *Escherichia coli*. *Protein Expr Purif* 51: 283-292, 2007.
5. Hanner M, Moebius FF, Flandorfer A, Knaus HG, Striessnig J, Kempner E and Glossmann H: Purification, molecular cloning, and expression of the mammalian sigma-1-binding site. *Proc Natl Acad Sci USA* 93: 8072-8077, 1996.
6. Penke B, Fulop L, Szucs M and Frecska E: The role of sigma-1 receptor, an intracellular chaperone in neurodegenerative diseases. *Curr Neuropharmacol* 16: 97-116, 2018.
7. Maurice T, Strehaiano M, Duhr F and Chevallier N: Amyloid toxicity is enhanced after pharmacological or genetic invalidation of the  $\sigma_1$  receptor. *Behav Brain Res* 339: 1-10, 2018.
8. Jia H, Zhang Y and Huang Y: Imaging sigma receptors in the brain: New opportunities for diagnosis of Alzheimer's disease and therapeutic development. *Neurosci Lett* 691: 3-10, 2019.
9. Wang L, Prescott AR, Spruce BA, Sanderson J and Duncan G: Sigma receptor antagonists inhibit human lens cell growth and induce pigmentation. *Invest Ophthalmol Vis Sci* 46: 1403-1408, 2005.
10. Bucolo C, Drago F, Lin LR and Reddy VN: Sigma receptor ligands protect human retinal cells against oxidative stress. *Neuroreport* 17: 287-291, 2006.
11. Morihara R, Yamashita T, Liu X, Nakano Y, Fukui Y, Sato K, Ohta Y, Hishikawa N, Shang J and Abe K: Protective effect of a novel sigma-1 receptor agonist is associated with reduced endoplasmic reticulum stress in stroke male mice. *J Neurosci Res* 96: 1707-1716, 2018.
12. Omi T, Tanimukai H, Kanayama D, Sakagami Y, Tagami S, Okochi M, Morihara T, Sato M, Yanagida K, Kitasyoji A, *et al*: Fluvoxamine alleviates ER stress via induction of Sigma-1 receptor. *Cell Death Dis* 5: e1332, 2014.
13. Demirtas L, Guclu A, Erdur FM, Akbas EM, Ozcicek A, Onk D and Turkmen K: Apoptosis, autophagy & endoplasmic reticulum stress in diabetes mellitus. *Indian J Med Res* 144: 515-524, 2016.
14. Eizirik DL, Pasquali L and Cnop M: Pancreatic  $\beta$ -cells in type 1 and type 2 diabetes mellitus: different pathways to failure. *Nat Rev Endocrinol* 16: 349-362, 2020.
15. Livak KJ and Schmittgen TD: Analysis of relative gene expression data using real-time quantitative PCR and the 2(-Delta Delta C(T)) method. *Methods* 25: 402-408, 2001.
16. Shi X, Deng H, Dai Z, Xu Y, Xiong X, Ma P and Cheng J: Nr2e1 deficiency augments palmitate-induced oxidative stress in beta cells. *Oxid Med Cell Longev* 2016: 9648769, 2016.
17. Dingreville F, Panthou B, Thivolet C, Ducreux S, Gouriou Y, Pesenti S, Chauvin MA, Chikh K, Errazuriz-Cerda E, Van Coppenolle F, *et al*: Differential effect of glucose on ER-Mitochondria  $\text{Ca}^{2+}$  exchange participates in insulin secretion and glucotoxicity-mediated dysfunction of  $\beta$ -cells. *Diabetes* 68: 1778-1794, 2019.
18. Hetz C and Papa FR: The unfolded protein response and cell fate control. *Mol Cell* 69: 169-181, 2018.
19. Baehr LM, West DW, Marcotte G, Marshall AG, De Sousa LG, Baar K and Bodine SC: Age-related deficits in skeletal muscle recovery following disuse are associated with neuromuscular junction instability and ER stress, not impaired protein synthesis. *Aging (Albany NY)* 8: 127-146, 2016.
20. B   A: Alcohol and thiamine deficiency trigger differential mitochondrial transition pore opening mediating cellular death. *Apoptosis* 22: 741-752, 2017.

21. Filadi R, Theurey P and Pizzo P: The endoplasmic reticulum-mitochondria coupling in health and disease: Molecules, functions and significance. *Cell Calcium* 62: 1-15, 2017.
22. Sasi USS, Ganapathy S, Palayyan SR and Gopal RK: Mitochondria associated membranes (MAMs): Emerging drug targets for diabetes. *Curr Med Chem* 27: 3362-3385, 2020.
23. Kim FJ: Introduction to Sigma proteins: Evolution of the concept of Sigma receptors. *Handb Exp Pharmacol* 244: 1-11, 2017.
24. Alenzi FQ: Links between apoptosis, proliferation and the cell cycle. *Br J Biomed Sci* 61: 99-102, 2004.
25. Ojo OO, Srinivasan DK, Owolabi BO, Conlon JM, Flatt PR and Abdel-Wahab YH: Magainin-AM2 improves glucose homeostasis and beta cell function in high-fat fed mice. *Biochim Biophys Acta* 1850: 80-87, 2015.
26. Cnop M, Abdulkarim B, Bottu G, Cunha DA, Igoillo-Esteve M, Masini M, Turatsinze JV, Griebel T, Villate O, Santin I, *et al*: RNA sequencing identifies dysregulation of the human pancreatic islet transcriptome by the saturated fatty acid palmitate. *Diabetes* 63: 1978-1993, 2014.
27. Zhai M, Liu C, Li Y, Zhang P, Yu Z, Zhu H, Zhang L, Zhang Q, Wang J and Wang J: Dexmedetomidine inhibits neuronal apoptosis by inducing Sigma-1 receptor signaling in cerebral ischemia-reperfusion injury. *Aging (Albany NY)* 11: 9556-9568, 2019.
28. Shinoda Y, Haga Y, Akagawa K and Fukunaga K: Wildtype  $\sigma 1$  receptor and the receptor agonist improve ALS-associated mutation-induced insolubility and toxicity. *J Biol Chem* 295: 17573-17587, 2020.
29. Rutter GA and Pinton P: Mitochondria-associated endoplasmic reticulum membranes in insulin signaling. *Diabetes* 63: 3163-3165, 2014.
30. Ono Y, Tanaka H, Tsuruma K, Shimazawa M and Hara H: A sigma-1 receptor antagonist (NE-100) prevents tunicamycin-induced cell death via GRP78 induction in hippocampal cells. *Biochem Biophys Res Commun* 434: 904-909, 2013.
31. Zhong S, Ye W, Lin SH, Liu JY, Leong J, Ma C and Lin YC: Zeranin induces cell proliferation and protein disulfide isomerase expression in mammary gland of ACI rat. *Anticancer Res* 31: 1659-1665, 2011.
32. Smith SB, Wang J, Cui X, Mysona BA, Zhao J and Bollinger KE: Sigma 1 receptor: A novel therapeutic target in retinal disease. *Prog Retin Eye Res* 67: 130-149, 2018.
33. Shioda N, Ishikawa K, Tagashira H, Ishizuka T, Yawo H and Fukunaga K: Expression of a truncated form of the endoplasmic reticulum chaperone protein,  $\sigma 1$  receptor, promotes mitochondrial energy depletion and apoptosis. *J Biol Chem* 287: 23318-23331, 2012.
34. Tagashira H, Bhuiyan MS and Fukunaga K: Diverse regulation of IP3 and ryanodine receptors by pentazocine through  $\sigma 1$ -receptor in cardiomyocytes. *Am J Physiol Heart Circ Physiol* 305: H1201-H1212, 2013.
35. Marchi S, Patergnani S and Pinton P: The endoplasmic reticulum-mitochondria connection: one touch, multiple functions. *Biochim Biophys Acta* 1837: 461-469, 2014.
36. Hedskog L, Pinho CM, Filadi R, Rönnbäck A, Hertwig L, Wiehager B, Larssen P, Gellhaar S, Sandebring A, Westerlund M, *et al*: Modulation of the endoplasmic reticulum-mitochondria interface in Alzheimer's disease and related models. *Proc Natl Acad Sci USA* 110: 7916-7921, 2013.
37. Rückl M, Parker I, Marchant JS, Nagaiah C, Jochenning FW and Rüdiger S: Modulation of elementary calcium release mediates a transition from puffs to waves in an IP3R cluster model. *PLoS Comput Biol* 11: e1003965, 2015.
38. Janikiewicz J, Szymański J, Malinska D, Patalas-Krawczyk P, Michalska B, Duszyński J, Giorgi C, Bonora M, Dobrzyn A and Wieckowski MR: Mitochondria-associated membranes in aging and senescence: structure, function, and dynamics. *Cell Death Dis* 9: 332, 2018.
39. Kerkhofs M, Bultynck G, Vervliet T and Monaco G: Therapeutic implications of novel peptides targeting ER-mitochondria  $\text{Ca}^{2+}$ -flux systems. *Drug Discov Today* 24: 1092-1103, 2019.
40. Bravo R, Vicencio JM, Parra V, Troncoso R, Munoz JP, Bui M, Quiroga C, Rodriguez AE, Verdejo HE, Ferreira J, *et al*: Increased ER-mitochondrial coupling promotes mitochondrial respiration and bioenergetics during early phases of ER stress. *J Cell Sci* 124: 2143-2152, 2011.
41. Hayashi T: The Sigma-1 receptor in cellular stress signaling. *Front Neurosci* 13: 733, 2019.



This work is licensed under a Creative Commons Attribution-NonCommercial-NoDerivatives 4.0 International (CC BY-NC-ND 4.0) License.